



TECHNICAL UNIVERSITY OF CRETE

SCHOOL OF ELECTRONIC AND COMPUTER ENGINEERING

Optimal Blind Detection of APSK
in Polynomial Time

A thesis submitted in partial fulfillment of the requirements for the
Master of Science of Electronic and Computer Engineering.

Author

Yannis Fountzoulas

Thesis Committee

Assoc. Prof. George N. Karystinos (advisor)

Assoc. Prof. Aggelos Bletsas

Assist. Prof. Dimitris-Alexandros Toumpakaris

Chania, October 2014

Abstract

Amplitude/phase-shift keying (APSK) is a power and bandwidth-efficient modulation technique that is robust against high-power-amplifier nonlinear distortion effects and has been adopted in the standard DVB-S2 for digital video broadcasting and interactive broadband satellite services. Differential APSK has been studied as a simple noncoherent alternative that avoids channel estimation and tracking at the receiver. However, if the channel is unknown at the receiver end, then the optimal blind detector takes the form of a sequence detector and has exponential (in the sequence length) complexity when implemented through a conventional exhaustive search among all possible data sequences. In this work, we develop a novel algorithm that has polynomial complexity and performs optimal blind sequence detection of APSK.

Contents

1	Introduction	5
2	Problem Statement	8
3	Polynomial-Complexity Optimal M-APSK Sequence Detection	10
3.1	A polynomial number of subproblems	11
3.2	Utilizing the auxiliary-angle technique	13
3.3	The case of $L = 2$	14
4	The Proposed Algorithm	22
5	Extension to the general case of $L > 2$	25
6	Simulation Results	27
7	Appendix	29

1 Introduction

Amplitude/phase-shift keying (APSK) is a power- and bandwidth-efficient modulation technique that combines characteristics of phase-shift keying (PSK) and quadrature amplitude modulation (QAM), is robust against high-power-amplifier nonlinear distortion effects, and attains nearly-QAM and nearly-PSK performance in linear and nonlinear, respectively, channels [1–14]. As such, APSK (or star-QAM) has been adopted in the standard DVB-S2 for digital video broadcasting and interactive broadband satellite services [1, 2, 5, 7, 8, 14].

A simple modification of APSK that avoids the need for channel estimation and tracking is differential APSK (DAPSK) [2–4, 6, 7, 9–13] in conjunction with conventional one-lag (symbol-by-symbol) processing at the receiver end. Nevertheless, the lack of channel knowledge at the receiver induces memory in the received sequence and single-symbol detection is no longer optimal; instead, maximum-likelihood (ML) sequence detection over the channel coherence period has to be performed for error rate minimization. This was first identified in [15–18] where it was shown that ML blind sequence detection offers significant performance gain over conventional single-symbol blind detection in terms of error rate; as the sequence length increases, the gain becomes larger and the performance of the blind sequence detector attains that of the coherent detector. This gain translates into capacity increase as was pointed out in [19, 20]. Moreover, in [4], it was shown that conventional PSK and QAM suffice to approach the unconstrained capacity in the single-input single-output (SISO) block Rayleigh-fading channel.

In general, optimal sequence detection has a great disadvantage in comparison to conventional (suboptimal) single-symbol detection; it requires an exhaustive search among all candidate sequences (i.e., sequences that are valid transmit sequences according to the adopted modulation scheme). Hence, its complexity is (in general) exponential in the sequence length. However, there are cases where such a search is avoided because the optimal detector can be implemented by efficient polynomial-complexity algorithms. The first such algorithm appeared in [21, 22]; it performs optimal blind detection of a sequence of PSK symbols over a quasi-static Rayleigh flat-fading channel with only log-linear complexity. The development of the algorithm in [21, 22] is based on the auxiliary-angle technique that was introduced therein and used afterwards in [23–25].

In addition to PSK, fast algorithms for optimal blind sequence detection in other linear-modulation

cases have also appeared over the past years. The log-linear-complexity algorithm that was presented in [26] performs generalized-likelihood-ratio-test (GLRT) sequence detection for PAM or rectangular-QAM transmissions over a phase-noncoherent channel (i.e., known channel amplitude). On the other hand, for the amplitude-noncoherent channel, a log-linear-complexity algorithm for GLRT-optimal detection of PAM or rectangular-QAM was developed in [27]. The work in [27] used lattice-decoding techniques and also presented a GLRT-optimal algorithm (for the case of unknown channel amplitude and phase) with cubic complexity; the complexity was further reduced to log-quadratic in [28]. A ML-optimal algorithm for blind detection of PAM or rectangular-QAM symbol sequences under Rayleigh fading with polynomial complexity was developed in [29]. All the above algorithms are restricted to square and rectangular QAM constellations (i.e., constellations with independent in-phase and quadrature components). In an attempt to treat the nonrectangular-QAM case, a suboptimal algorithm of log-quadratic complexity for blind detection of hexagonal QAM was presented in [30]. The approach in [30] is similar to the one in [27], with hypercubes having been replaced by polytopes.

The case of APSK does not fall into any of the above studies, mainly because the in-phase and quadrature components are no longer independent. Hence, efficient algorithms for optimal blind sequence detection of APSK cannot be derived from the above works. Blind detection of APSK has been considered in [2] in conjunction with differential encoding but suboptimal sequence decoding. In [13], differential encoding based on a look-up table instead of a rule for QAM and APSK is proposed and shown to outperform conventional differential encoding [2]. Further performance improvements have been attempted with the assistance of channel coding in [9–12]. Nevertheless, until today, the only known algorithm that performs ML- or GLRT-optimal blind sequence detection of APSK is the conventional exhaustive-search approach whose complexity is exponential in the sequence length.

In this work, we develop an algorithm for GLRT blind detection of APSK symbol sequences under flat fading whose complexity is polynomial in the sequence length. The proposed algorithm is also ML-optimal when the channel distribution is Rayleigh. Our approach utilizes the decomposition that was used in [29] for the case of PAM and rectangular QAM to create a polynomial-size set of simple subproblems. For each subproblem, we use the auxiliary-angle approach which, in principle, rephrases a computationally-hard exhaustive-search problem into one that has to run on a polynomial-size search set. This new set is shown to include the optimal sequence for the subproblem and is built with polynomial complexity by the proposed algorithm. Hence, through the proposed algorithm, the

GLRT-optimal sequence (or ML-optimal sequence under Rayleigh fading) is computed with polynomial complexity.

The rest of this thesis is organized as follows. In Section 2, the problem formulation is provided and in Section 3 the proposed method is presented. In Section 4, we present a detailed description of the proposed algorithm for optimal blind sequence detection of APSK, as well as the corresponding pseudo-code. In Section 5, we extend the proposed method for the general case, since Section 3 is tailored to a subclass of the original problem for presentation simplicity. Finally, Section 6 illustrates the performance of the proposed method through simulations.

2 Problem Statement

We consider a SISO system and assume transmission of a length- N sequence $\mathbf{s} = [s_1, s_2, \dots, s_N]^T$ of M -APSK data symbols where each symbol s_n , $n = 1, 2, \dots, N$, is selected from a constellation $\mathcal{A} \triangleq \bigcup_{l=1}^L \mathcal{A}_l(\theta)$ and

$$\mathcal{A}_l(\theta) \triangleq \begin{cases} \{r_l \exp(j(\frac{2\pi k}{M} + \theta)) \mid k = 1, 3, 5, \dots\} & , \text{ if } l \text{ even} \\ \{r_l \exp(j(\frac{2\pi k}{M} + \theta)) \mid k = 0, 2, 4, \dots\} & , \text{ if } l \text{ odd.} \end{cases} \quad (1)$$

In (1), L is the number of APSK circles (amplitude levels), θ is a constant arbitrary phase in $[0, 2\pi)$, and, $\forall l = 1, 2, \dots, L$, $|\mathcal{A}_l(\theta)| = \frac{M}{L}$ and $r_l \in \mathbb{R}_+$. We also assume that $0 < r_1 < r_2 < \dots < r_L$, without loss of generality. The above definition produces constellations like those in Fig. 1 and any rotated version of them. The data sequence is shaped, upconverted, and transmitted over a flat-fading channel whose coherence period is at least N symbol periods. At the destination, after downconversion and pulse-matched filtering, the received vector is

$$\mathbf{y} = h\mathbf{s} + \mathbf{n} \quad (2)$$

where h is a complex channel coefficient and $\mathbf{n} \sim \mathcal{CN}(\mathbf{0}, \sigma_n^2 \mathbf{I})$ denotes zero-mean additive white complex Gaussian noise.

In this work, we assume that the channel coefficient h is not available to the receiver. Therefore, coherent detection cannot be utilized and the optimal, in terms of sequence error rate, receiver takes the form of a sequence detector that operates on the entire received vector \mathbf{y} .¹ Given the observation vector \mathbf{y} , the ML detector for the M -APSK sequence \mathbf{s} maximizes the conditional probability density function (pdf) of \mathbf{y} given \mathbf{s} . Thus, the optimal decision is given by

$$\mathbf{s}^{\text{ML}} = \arg \max_{\mathbf{s} \in \mathcal{A}^N} f(\mathbf{y}|\mathbf{s}) \quad (3)$$

where $f(\cdot|\cdot)$ represents the pertinent vector pdf of the channel output conditioned on the transmitted symbol sequence. If the fading distribution is Rayleigh, i.e., $h \sim \mathcal{CN}(0, \sigma_h^2)$, then the conditional

¹In the following, for brevity, we refer to sequence-error-rate optimal detection simply as optimal.

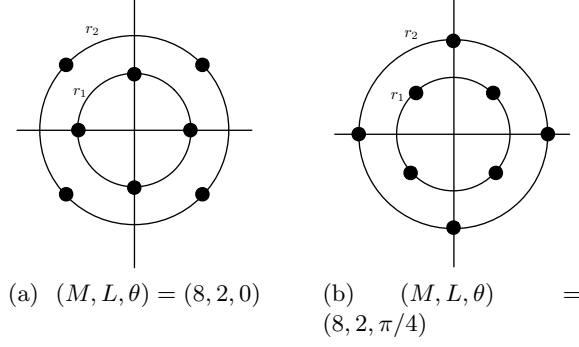


Figure 1: Examples of constellations considered in this thesis.

received vector \mathbf{y} given the transmitted sequence \mathbf{s} is a complex Gaussian vector with mean $E\{\mathbf{y}|\mathbf{s}\} = \mathbf{0}_{N \times 1}$ and covariance matrix

$$\mathbf{C}_{\mathbf{y}|\mathbf{s}} \triangleq E\{\mathbf{y}\mathbf{y}^H|\mathbf{s}\} = \sigma_h^2 \mathbf{s}\mathbf{s}^H + \sigma_n^2 \mathbf{I}_N. \quad (4)$$

Therefore, the ML optimization problem in (3) is rewritten as

$$\mathbf{s}^{\text{ML}} = \arg \max_{\mathbf{s} \in \mathcal{A}^N} \frac{1}{|\mathbf{C}_{\mathbf{y}|\mathbf{s}}|} \exp\left(-\mathbf{y}^H \mathbf{C}_{\mathbf{y}|\mathbf{s}}^{-1} \mathbf{y}\right) \quad (5)$$

Using identities for the determinant and inverse of a rank-1 update [31], we compute

$$|\mathbf{C}_{\mathbf{y}|\mathbf{s}}| = |\sigma_n^2 \mathbf{I}_N + \sigma_h^2 \mathbf{s}\mathbf{s}^H| = |\sigma_n^2 \mathbf{I}_N| \left(1 + \frac{\sigma_h^2}{\sigma_n^2} \|\mathbf{s}\|^2\right) = \sigma_n^{2N-2} (\sigma_n^2 + \sigma_h^2 \|\mathbf{s}\|^2) \quad (6)$$

and

$$\mathbf{C}_{\mathbf{y}|\mathbf{s}}^{-1} = (\sigma_n^2 \mathbf{I}_N + \sigma_h^2 \mathbf{s}\mathbf{s}^H)^{-1} = \frac{1}{\sigma_n^2} \mathbf{I}_N - \frac{\sigma_h^2}{\sigma_n^4 + \sigma_h^2 \sigma_n^2 \|\mathbf{s}\|^2} \mathbf{s}\mathbf{s}^H. \quad (7)$$

Substituting (6) and (7) in (5), we obtain

$$\begin{aligned} \mathbf{s}^{\text{ML}} &= \arg \max_{\mathbf{s} \in \mathcal{A}^N} \left\{ -\mathbf{y}^H \left(\frac{1}{\sigma_n^2} \mathbf{I}_N - \frac{\sigma_h^2}{\sigma_n^4 + \sigma_h^2 \sigma_n^2 \|\mathbf{s}\|^2} \mathbf{s}\mathbf{s}^H \right) \mathbf{y} - \ln(\sigma_n^2 + \sigma_h^2 \|\mathbf{s}\|^2) \right\} \\ &= \arg \max_{\mathbf{s} \in \mathcal{A}^N} \left\{ \frac{\sigma_h^2}{\sigma_n^2 (\sigma_h^2 \|\mathbf{s}\|^2 + \sigma_n^2)} |\mathbf{y}^H \mathbf{s}|^2 - \ln(\sigma_n^2 + \sigma_h^2 \|\mathbf{s}\|^2) \right\} \\ &= \arg \max_{\mathbf{s} \in \mathcal{A}^N} \left\{ g_{\text{ML}}(\|\mathbf{s}\|) |\mathbf{y}^H \mathbf{s}|^2 + h_{\text{ML}}(\|\mathbf{s}\|) \right\} \end{aligned} \quad (8)$$

where $g_{\text{ML}}(x) \triangleq \frac{\sigma_h^2}{\sigma_n^2 (\sigma_h^2 x^2 + \sigma_n^2)}$ and $h_{\text{ML}}(x) \triangleq -\ln(\sigma_n^2 + \sigma_h^2 x^2)$.

If, on the other hand, the channel distribution is not Rayleigh or is unknown, then we may consider joint channel estimation and data detection and the GLRT rule [27], [28]

$$\mathbf{s}^{\text{GLRT}} = \arg \min_{\mathbf{s} \in \mathcal{A}^N} \left\{ \min_{h \in \mathbb{C}} \|\mathbf{y} - h\mathbf{s}\| \right\} = \arg \min_{\mathbf{s} \in \mathcal{A}^N} \left\| \mathbf{y} - \frac{\mathbf{s}^H \mathbf{y}}{\|\mathbf{s}\|^2} \mathbf{s} \right\| = \arg \max_{\mathbf{s} \in \mathcal{A}^N} \frac{|\mathbf{y}^H \mathbf{s}|^2}{\|\mathbf{s}\|^2} \quad (9)$$

which, similarly to (5), can take the form

$$\mathbf{s}^{\text{GLRT}} = \arg \max_{\mathbf{s} \in \mathcal{A}^N} \left\{ g_{\text{GLRT}}(\|\mathbf{s}\|) |\mathbf{y}^H \mathbf{s}|^2 + h_{\text{GLRT}}(\|\mathbf{s}\|) \right\} \quad (10)$$

by setting $g_{\text{GLRT}}(x) \triangleq \frac{1}{x^2}$ and $h_{\text{GLRT}}(x) \triangleq 0$.

Hence, both the ML optimization problem in (5) and the GLRT optimization problem in (9) are special cases of the more general optimization problem

$$\boxed{\mathcal{P} : \max_{\mathbf{s} \in \mathcal{A}^N} \left\{ g(\|\mathbf{s}\|) |\mathbf{y}^H \mathbf{s}|^2 + h(\|\mathbf{s}\|) \right\}} \quad (11)$$

where $g : \mathbb{R} \rightarrow \mathbb{R}_+$ and $h : \mathbb{R} \rightarrow \mathbb{R}$.

A straightforward approach to solve \mathcal{P} would be an exhaustive search among all M^N sequences $\mathbf{s} \in \mathcal{A}^N$. However, such a solver would be impractical even for moderate values of N , since its complexity grows exponentially with N . In the next section, we present an efficient algorithm that solves \mathcal{P} in polynomial time for any $g : \mathbb{R} \rightarrow \mathbb{R}_+$ and $h : \mathbb{R} \rightarrow \mathbb{R}$.

3 Polynomial-Complexity Optimal M -APSK Sequence Detection

The main contribution of this work is stated in the following proposition.

Proposition 1 *Problem \mathcal{P} is solvable with complexity polynomial in N .* □

We follow a proof-by-construction which we decompose into the following parts. First, we show that \mathcal{P} is equivalent to a union of subproblems whose number is polynomial in N . Then, we show that,

for each subproblem, we can identify a set of candidate solutions which includes the solution of the subproblem, has cardinality polynomial in N , and can be built in time polynomial in N . Hence, the solution of \mathcal{P} is always in this ensemble of candidate sets, implying that the aggregate complexity to solve \mathcal{P} is polynomial in N .

3.1 A polynomial number of subproblems

We start by defining the supersets \mathcal{B} and \mathcal{X} which contain all possible amplitude and phase, respectively, values of the APSK constellation, that is,

$$\mathcal{B} \triangleq \bigcup_{l=1}^L \mathcal{B}_l \text{ where } \mathcal{B}_l \triangleq \{r_l\} \quad (12)$$

and

$$\mathcal{X} \triangleq \bigcup_{l=1}^L \mathcal{X}_l \text{ where } \mathcal{X}_l \triangleq \{\underline{\angle} \mathbf{s} : \mathbf{s} \in \mathcal{A}_l(\theta)\}, \quad (13)$$

where $\underline{\angle} \mathbf{s}$ denotes the angle of \mathbf{s} in radians. We observe that, if $|s| \in \mathcal{B}_l$ for some $l = 1, 2, \dots, L$, then $\underline{\angle} s$ belongs to the corresponding subset \mathcal{X}_l . In other words, every APSK symbol $s \in \mathcal{A}$ can be seen as a combination of elements, say $b \in \mathcal{B}$ and $x \in \mathcal{X}$, such that if $b \in \mathcal{B}_l$ for a specific l , then $x \in \mathcal{X}_l$ for the same l . That is, $s = be^{jx}$.

Similarly, we may view each APSK sequence $\mathbf{s} \in \mathcal{A}^N$ as a combination of vectors $\mathbf{b} \in \mathcal{B}^N$ and $\mathbf{x} \in \mathcal{X}^N$, so that $\mathbf{s} = \mathbf{b} \odot e^{j\mathbf{x}}$ and $\|\mathbf{s}\| = \|\mathbf{b}\|$, where \odot accounts for entry-wise product. Then, we can rewrite \mathcal{P} in (11) as

$$\max_{\mathbf{b} \in \mathcal{B}^N} \max_{\mathbf{x} \in \mathcal{X}^N} \left\{ g(\|\mathbf{b}\|) |\mathbf{y}^H (\mathbf{b} \odot e^{j\mathbf{x}})|^2 + h(\|\mathbf{b}\|) \right\}. \quad (14)$$

Hence, instead of searching for the optimal $\mathbf{s} \in \mathcal{A}^N$ in (11), we search for the optimal amplitude-phase pair $(\mathbf{b}, \mathbf{x}) \in \mathcal{B}^N \times \mathcal{X}^N$ in (14).

The main idea that we exploit and which eventually leads to a tractable and efficient algorithm is the following. If we fix the type [32] of sequence \mathbf{b} (i.e., the frequency of appearance of the elements of \mathcal{B} in \mathbf{b}), then the norm of \mathbf{b} is also fixed and the double maximization problem in (14) takes a simpler form which is solvable in polynomial time. Interestingly, the number of all possible types is polynomial in N , leading to a polynomial-time solution of (14).

To formulate our approach, we define function F which associates any vector $\mathbf{b} \in \mathcal{B}^N$ to its

unnormalized type vector $\mathbf{t} = F(\mathbf{b}) \in \{0, 1, \dots, N\}^L$. That is, the m th element t_m of $\mathbf{t} = F(\mathbf{b})$ equals the number of times of appearance of value r_m in \mathbf{b} , $m = 1, 2, \dots, L$. Then, we partition \mathcal{B}^N into disjoint sets $\mathcal{B}^{(0)}, \mathcal{B}^{(1)}, \dots, \mathcal{B}^{(K)}$ so that each set $\mathcal{B}^{(k)}$ contains all vectors $\mathbf{b} \in \mathcal{B}^N$ with common type, say \mathbf{t}_k , and, hence, common norm, say β_k . More formally,

$$\mathcal{B}^N = \bigcup_{k=0}^K \mathcal{B}^{(k)} \quad (15)$$

where, for any $k = 0, 1, \dots, K$,

$$\mathcal{B}^{(k)} \triangleq \{\mathbf{b} \in \mathcal{B}^N : \|\mathbf{b}\| = \beta_k\}. \quad (16)$$

Apparently, the number $K + 1$ of all distinct types (hence, sets) equals the number of possible ways one can choose N elements of a set of L elements, disregarding order and allowing repeated elements, and is given by [33]

$$K + 1 = \binom{L + N - 1}{N}. \quad (17)$$

As a result, $K + 1 = \mathcal{O}(N^{L-1})$ which is polynomial in N .

Since we have partitioned \mathcal{B}^N into $K + 1$ sets so that each set contains vectors with common type and norm, using (14) we can re-express \mathcal{P} as

$$\begin{aligned} & \max_{k=0,1,\dots,K} \max_{\mathbf{b} \in \mathcal{B}^{(k)}} \left\{ g(\|\mathbf{b}\|) \max_{\mathbf{x} \in \mathcal{X}^N} |\mathbf{y}^H (\mathbf{b} \odot \mathbf{e}^{j\mathbf{x}})|^2 + h(\|\mathbf{b}\|) \right\} \\ & = \max_{k=0,1,\dots,K} \max_{\mathbf{b} \in \mathcal{B}^{(k)}} \left\{ g(\beta_k) \max_{\mathbf{x} \in \mathcal{X}^N} |\mathbf{y}^H (\mathbf{b} \odot \mathbf{e}^{j\mathbf{x}})|^2 + h(\beta_k) \right\} \end{aligned} \quad (18)$$

According to (18), to obtain the optimal pair $(\mathbf{b}, \mathbf{x}) \in \mathcal{B}^N \times \mathcal{X}^N$, we can equivalently compute the optimal pair $(\mathbf{b}, \mathbf{x}) \in \mathcal{B}^{(k)} \times \mathcal{X}^N$, for each $k = 0, 1, \dots, K$. That is, we can focus on the innermost maximization in (18),

$$\max_{\mathbf{b} \in \mathcal{B}^{(k)}} \max_{\mathbf{x} \in \mathcal{X}^N} |\mathbf{y}^H (\mathbf{b} \odot \mathbf{e}^{j\mathbf{x}})|^2 \quad (19)$$

or, simply, focus on

$$\boxed{\mathcal{P}_k : \max_{\mathbf{b} \in \mathcal{B}^{(k)}} \max_{\mathbf{x} \in \mathcal{X}^N} |\mathbf{y}^H (\mathbf{b} \odot \mathbf{e}^{j\mathbf{x}})|} \quad (20)$$

Hence, we have the following lemma.

Lemma 1 Solving the $K + 1 = \mathcal{O}(N^{L-1})$ subproblems $\mathcal{P}_0, \mathcal{P}_1, \dots, \mathcal{P}_K$ is sufficient to solve \mathcal{P} . \square

3.2 Utilizing the auxiliary-angle technique

To develop an efficient method for solving \mathcal{P}_k and, equivalently, \mathcal{P} , we rely on the auxiliary-angle technique that was introduced in [21, 22] and also used in [23–25]. We utilize the fact that

$$|\mathbf{y}^H (\mathbf{b} \odot e^{j\mathbf{x}})| = \max_{\phi \in [0, 2\pi)} \left(-\Im \left\{ e^{-j\phi} (\mathbf{b} \odot e^{j\mathbf{x}})^H \mathbf{y} \right\} \right). \quad (21)$$

Therefore, by applying (21) to (20), \mathcal{P}_k is equivalent to

$$\max_{\mathbf{b} \in \mathcal{B}^{(k)}} \max_{\mathbf{x} \in \mathcal{X}^N} \max_{\phi \in [0, 2\pi)} \left(-\Im \left\{ e^{-j\phi} (\mathbf{b} \odot e^{j\mathbf{x}})^H \mathbf{y} \right\} \right) \quad (22)$$

which can be rewritten as

$$\max_{\phi \in [0, 2\pi)} \max_{\mathbf{b} \in \mathcal{B}^{(k)}} \max_{\mathbf{x} \in \mathcal{X}^N} - \sum_{n=1}^N b_n \Im \left\{ y_n e^{-j(x_n + \phi)} \right\}. \quad (23)$$

We can reduce the overall complexity restricting to the range of the auxiliary angle from $\Phi = [0, 2\pi)$ to $[0, \frac{4\pi}{M})$ without losing optimality in (23), according to the following lemma.

Lemma 2 It is sufficient to examine the range $[0, \frac{4\pi}{M})$ instead of $[0, 2\pi)$.

Proof: Suppose that for a certain $\phi \in [0, \frac{4\pi}{M})$ we obtain the optimal pair $(\mathbf{b}, \mathbf{x}) \in \mathcal{B}^{(k)} \times \mathcal{X}^N$. Using (23) we result in the following metric value

$$- \sum_{n=1}^N b_n \Im \left\{ y_n e^{-j(x_n + \phi)} \right\}. \quad (24)$$

Consider a phase shifting by $\frac{4\pi}{M}$ (i.e., $\phi' = \phi + \frac{4\pi}{M} \in [\frac{4\pi}{M}, \frac{8\pi}{M})$). Substituting in (23) for the given ϕ' we obtain

$$\begin{aligned} & \max_{\mathbf{b}' \in \mathcal{B}^{(k)}} \max_{\mathbf{x}' \in \mathcal{X}^N} - \sum_{n=1}^N b'_n \Im \left\{ y_n e^{-j(x'_n + \phi')} \right\} \\ &= \max_{\mathbf{b}' \in \mathcal{B}^{(k)}} \max_{\mathbf{x}' \in \mathcal{X}^N} - \sum_{n=1}^N b'_n \Im \left\{ y_n e^{-j((x'_n + \frac{4\pi}{M}) + \phi)} \right\}. \end{aligned}$$

But, for the above ϕ we know that the optimal pair is (\mathbf{b}, \mathbf{x}) . Thus, by setting $(\mathbf{b}', \mathbf{x}') = (\mathbf{b}, \mathbf{x} - \frac{4\pi}{M})$ we result in the same metric value. The proof is similar for $\phi' \in [\frac{8\pi}{M}, 2\pi)$, concluding that is sufficient to scan the range $[0, \frac{4\pi}{M})$ instead of the entire Φ . \blacksquare

3.3 The case of $L = 2$

We define

$$u_n(\phi) \triangleq b_n (\Re\{y_n\} \sin(x_n + \phi) + \Im\{y_n^*\} \cos(x_n + \phi)) \quad (25)$$

where $u_n(\phi)$ is a continuous function of ϕ , i.e., a curve in ϕ , and (23) can be written as

$$\max_{\phi \in [0, \frac{4\pi}{M})} \max_{\mathbf{b} \in \mathcal{B}^{(k)}} \max_{\mathbf{x} \in \mathcal{X}^N} \sum_{n=1}^N u_n(\phi). \quad (26)$$

From (17) we obtain that the number of subproblems that need to be solved are equal to $N + 1$. We will proceed as follows. First we find the candidate optimal pair $(\mathbf{b}, \mathbf{x}) \in \mathcal{B}^{(k)} \times \mathcal{X}^N$, $\forall k = 0, 1, \dots, K$, at $\phi = 0$ with complexity $\mathcal{O}(NM)$. We prove that, to select the next candidate optimal pair in each subproblem, we need $\mathcal{O}(N^2)$ time complexity and the cardinality of those pairs in each subproblem is $\mathcal{O}(N^2)$. Thus, we collect all the candidate optimal pairs for each subproblem with overall complexity $\mathcal{O}(N^4)$.² Consequently, we obtain the optimal pairs for the initial problem \mathcal{P} in (11) with complexity $\mathcal{O}(N^5)$.

At $\phi = 0$, equation (26) can be rewritten as

$$\max_{\mathbf{b} \in \mathcal{B}^{(k)}} \max_{\mathbf{x} \in \mathcal{X}^N} \sum_{n=1}^N u_n(0) = \max_{\mathbf{b} \in \mathcal{B}^{(k)}} \max_{\mathbf{x} \in \mathcal{X}^N} \sum_{n=1}^N b_n (\Re\{y_n\} \sin x_n + \Im\{y_n^*\} \cos x_n). \quad (27)$$

For $l = 1, 2$, we construct vectors $\mathbf{b}^{(l)} = [r_l, r_l, \dots, r_l]^T$, each of size $N \times 1$. Since each term of (27) is non negative, for the components of the optimal pair at $\phi = 0$, it is sufficient to maximize each term $u_n(0)$ instead of maximizing $\sum_{n=1}^N u_n(0)$. We denote this maximum value as $u_n^{\text{opt}}(0)$ and form the vector $\mathbf{u}^{(l)} = [u_1^{\text{opt}}(0), u_2^{\text{opt}}(0), \dots, u_N^{\text{opt}}(0)]^T$. Thus, for each $u_n(0)$ given the vector $\mathbf{b}^{(l)} \in \mathcal{B}_l^N$, we find the phase x_n that maximizes $u_n(0)$ through an exhaustive search in the set \mathcal{X}_l of cardinality $\frac{M}{2}$. Therefore, with complexity $\mathcal{O}(NM)$ we result in two triplets $(\mathbf{b}^{(l)}, \mathbf{x}^{(l)}, \mathbf{u}^{(l)})$. Next, we construct with complexity $\mathcal{O}(N)$ the vector $\mathbf{g} = \mathbf{u}^{(2)} - \mathbf{u}^{(1)}$. Intuitively, each term g_n of the vector \mathbf{g} indicates the

²As it will be shown later, the complexity is linear in N for subproblems \mathcal{P}_0 and \mathcal{P}_K .

gain we would have had if, instead of picking the point s_n with components $(b_n, x_n) \in \mathcal{B}_1 \times \mathcal{X}_1$, we had picked s_n with components $(b_n, x_n) \in \mathcal{B}_2 \times \mathcal{X}_2$. Therefore, we can sort the values of \mathbf{g} with complexity $\mathcal{O}(N \log N)$ and collect the indexes of the k greatest values (since we solve the \mathcal{P}_k subproblem). The optimal pair (\mathbf{b}, \mathbf{x}) for $\phi = 0$ is given if we set $(\mathbf{b}, \mathbf{x}) = (\mathbf{b}^{(1)}, \mathbf{x}^{(1)})$ and, in the k positions obtained in the previous step, we set the corresponding values from the vectors $(\mathbf{b}^{(2)}, \mathbf{x}^{(2)})$.

After we have obtained the optimal pair (\mathbf{b}, \mathbf{x}) at $\phi = 0$, we scan the interval $[0, \frac{4\pi}{M})$ to identify points where new candidate pairs are created. The general idea is the following. Since the optimal pair at $\phi = 0$ has been found, we form a polynomial (in N) number of sets $\mathcal{G}_1, \mathcal{G}_2, \dots$ to solve subproblems \mathcal{P}_k for $k = 1, 2, \dots, K - 1$. The cardinality of these sets is also polynomial in N and in each set we collect the ϕ 's in which the next candidate pair (\mathbf{b}, \mathbf{x}) is created considering phase-only changes or phase-and-amplitude changes on the current candidate pair. Among the ϕ 's in each set, we keep only one value of ϕ which will be denoted as $\phi^{(j)}$ for the corresponding set \mathcal{G}_j . The chosen $\phi^{(j)}$ for set \mathcal{G}_j satisfies the following constraints.

$$\begin{aligned} \phi^{(j)} &\leq \phi_k, \quad \forall k = 1, 2, \dots, |\mathcal{G}_j|, \\ \phi^{(j)} &> \phi^{(k)}, \quad \forall j > k, \text{ and} \\ \phi^{(j)} &\leq \frac{4\pi}{M}, \quad \forall j. \end{aligned} \tag{28}$$

To determine the cases that will lead us to the formation of a new candidate pair, we have to answer the following questions. What would have happened if, for some $n \in \{1, 2, \dots, N\}$, instead of the component $(b_n, x_n) \in \mathcal{B}_l \times \mathcal{X}_l$ for some fixed l , we had (b_n, x'_n) with $x'_n \in \mathcal{X}_l \setminus x_n$? Or, what would have happened if, for $i, j \in \{1, 2, \dots, N\}$ with $i \neq j$, instead of the components $(b_i, x_i) \in \mathcal{B}_1 \times \mathcal{X}_1$ and $(b_j, x_j) \in \mathcal{B}_2 \times \mathcal{X}_2$ we had $(b_j, x'_j) \in \mathcal{B}_2 \times \mathcal{X}_2$ and $(b_i, x'_i) \in \mathcal{B}_1 \times \mathcal{X}_1$, respectively? To better understand the above questions, the answers of which will constitute the backbone of the algorithm, we will proceed with an example.

Among subproblems \mathcal{P}_k , $k = 0, 1, \dots, K$, consider \mathcal{P}_0 (which is the simpler one). That is, all the symbols s_n , $\forall n = 1, 2, \dots, N$, lie on the circle with radius r_1 and the optimal pair at $\phi = 0$ has been obtained with the procedure described above. An example of solving subproblem \mathcal{P}_0 is illustrated in Fig. 3 for $N = 3$ and the corresponding curves $u_n(\phi)$, $n = 1, 2, 3$, are shown in Fig. 3a and Fig. 3b with solid lines. Since we can not exchange the amplitude components of the optimal pair, we consider only

phase changes. Consequently, we should calculate $\frac{M}{L} - 1$ phase changes, for each $n \in \{1, 2, \dots, N\}$. The quantity $\frac{M}{L} - 1$ is derived by considering the set $\mathcal{X}_1 \setminus x_n$ for each n . However, since we know the x_n 's, the calculation of the new $u_n(\phi)$ with components $(b_n, x'_n) \forall x'_n \in \mathcal{X}_1 \setminus x_n$ is needless. Instead, only the calculation of $u_n(\phi)$ with components $(b_n, x_n - \frac{4\pi}{M}) \forall n = 1, 2, \dots, N$, is necessary. The reason why only these terms lead to new candidate pairs can be interpreted geometrically as follows. Set, for example, $M = 8$ and consider a component (b_n, x_n) from the candidate pair (\mathbf{b}, \mathbf{x}) . The fact that the phase is x_n implies that s_n lies in either sector 1 or sector 2 in Fig. 2a. Since ϕ is taking values in the range $[0, \frac{\pi}{2})$, s_n will be rotated and will lie in either sector 3 or sector 4. In both cases, there is only one valid phase change, that is, a change by $\frac{\pi}{2}$. The above observation can be easily extended to an arbitrary M and, thus, we have to consider only the $u_n(\phi)$ with components $(b_n, x_n - \frac{4\pi}{M}) \forall n = 1, 2, \dots, N$.

The new $u_n(\phi)$, say $u'_n(\phi)$, that is formed by altering the component n of the candidate pair (\mathbf{b}, \mathbf{x}) from (b_n, x_n) to $(b_n, x_n - \frac{4\pi}{M})$, is also a curve in ϕ (it is shown in Fig. 3b with dotted lines for each n). When these two curves intersect at a point, say ϕ_n , the below observations are made.

1. Since (b_n, x_n) is a component of the optimal pair (\mathbf{b}, \mathbf{x}) , it is implied that, for the corresponding $u_n(\phi)$, we have $u_n(\phi) > u'_n(\phi)$ for any $u'_n(\phi)$ with components $(b_n, x'_n) \in \mathcal{B}_1 \times \{\mathcal{X}_1 \setminus x_n\}$, when $\phi < \phi_n$. Hence, $u_n(\phi)$ is also greater than $u'_n(\phi)$ with component $(b_n, x_n - \frac{4\pi}{M})$.
2. When $\phi > \phi_n$, the opposite is true. The new candidate optimal pair (\mathbf{b}, \mathbf{x}) is obtained from the previous one at $\phi = \phi_n$ by setting the n th component (b'_n, x'_n) equal to $(b_n, x_n - \frac{4\pi}{M})$.

The ϕ_n 's can be easily obtained by solving, with respect to ϕ , the equalities

$$u_n(\phi) = u_n\left(\phi - \frac{4\pi}{M}\right) \quad \forall n = 1, 2, \dots, N, \quad (29)$$

resulting in the N distinct values

$$\phi_n = \tan^{-1} \left(\frac{\Re\{y_n\}(\sin x_n - \sin(x_n - 4\pi/M)) + \Im\{y_n^*\}(\cos x_n - \cos(x_n - 4\pi/M))}{\Re\{y_n\}(\cos(x_n - 4\pi/M) - \cos x_n) + \Im\{y_n^*\}(\sin x_n - \sin(x_n - 4\pi/M))} \right), \quad \forall n = 1, 2, \dots, N. \quad (30)$$

of subproblem \mathcal{P}_0 , as illustrated in Fig. 3c. The construction of these pairs is accomplished in linear time. Thus, with complexity $\mathcal{O}(N)$, we compute N values of ϕ which correspond to the N candidate pairs. This implies that \mathcal{P}_0 is solvable in time $\mathcal{O}(N)$. In addition, notice that subproblem \mathcal{P}_K (i.e., all the points lie on the circle with radius r_2) is also solvable with the same complexity.

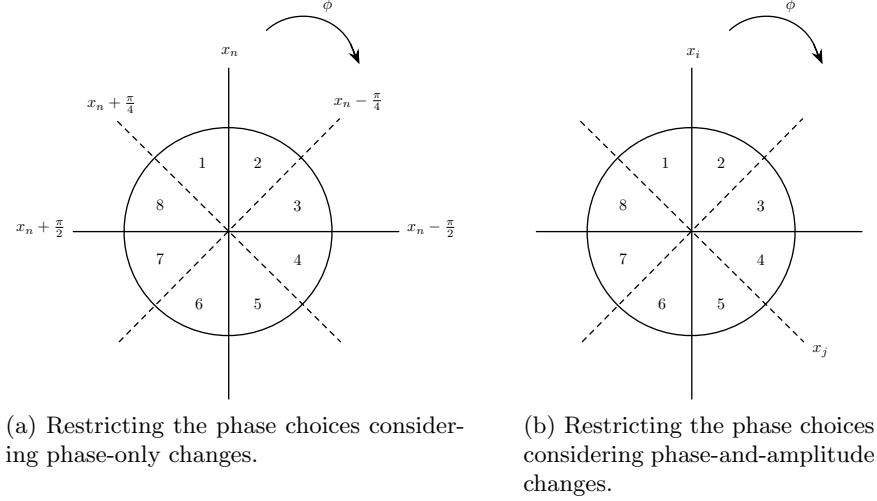
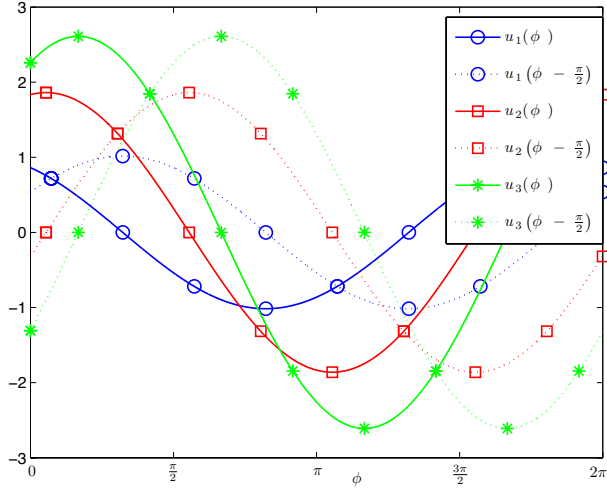


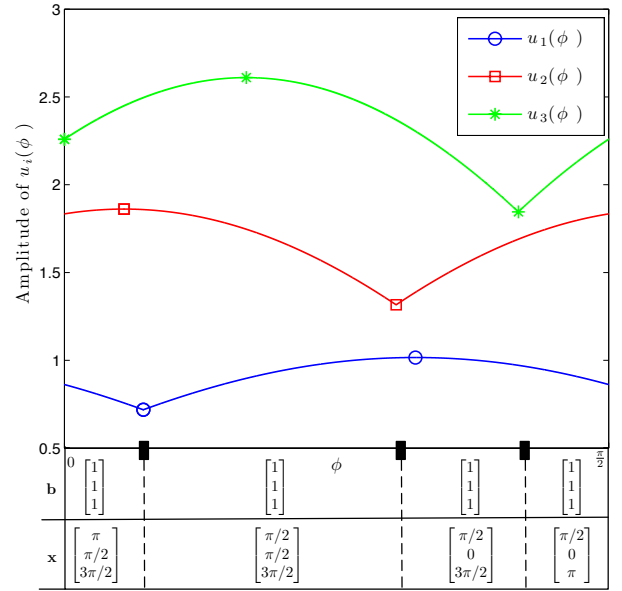
Figure 2: Partition Φ into sectors.

We proceed with the remaining subproblems \mathcal{P}_k , $k = 1, 2, \dots, K - 1$, and Fig. 4 illustrates an example of solving subproblem \mathcal{P}_1 . We obtain the optimal pair at $\phi = 0$ and the N values of ϕ_n 's from (30) with complexity $\mathcal{O}(N)$. In this case, any two components of the candidate pair, $(b_i, x_i) \in \mathcal{B}_1 \times \mathcal{X}_1$ and $(b_j, x_j) \in \mathcal{B}_2 \times \mathcal{X}_2$, with $b_i \neq b_j$, can swap positions. As a result, the new candidate pair $(\mathbf{b}', \mathbf{x}')$ has components $(b_j, x'_j) \in \mathcal{B}_2 \times \mathcal{X}_2$ and $(b_i, x'_i) \in \mathcal{B}_1 \times \mathcal{X}_1$, at the i th and j th, respectively, positions. The cardinality of the possible values of x'_i and x'_j can be restricted to four, instead of $\frac{M}{L}$. A geometric explanation similar to the case of the subproblem \mathcal{P}_0 follows. Since s_i has phase x_i , it is implied that it will lie in either sector 1 or sector 2 in Fig. 2b. Similarly, s_j will lie in either sector 4 or sector 5. Thus, on a phase-and-amplitude change, we obtain the following four combinations.

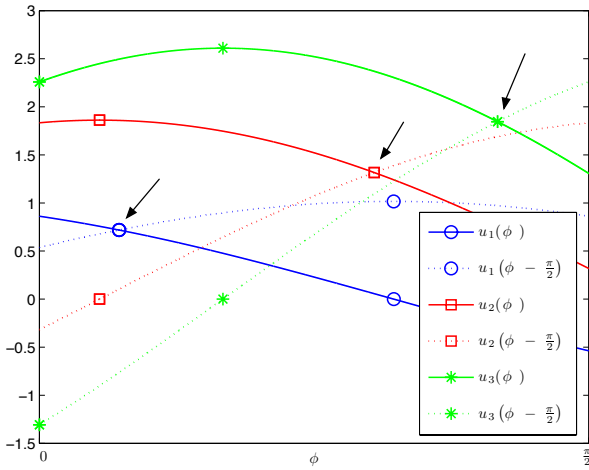
1. s_i in sector 1 and s_j in sector 4; therefore, in the new candidate pair, the i th and j th components will be $(b_j, x_i + \frac{\pi}{4})$ and $(b_i, x_j + \frac{\pi}{4})$ respectively.
2. s_i in sector 1 and s_j in sector 5; therefore, in the new candidate pair, the i th and j th components will be $(b_j, x_i + \frac{\pi}{4})$ and $(b_i, x_j - \frac{\pi}{4})$ respectively.
3. s_i in sector 2 and s_j in sector 4; therefore, in the new candidate pair, the i th and j th components will be $(b_j, x_i - \frac{\pi}{4})$ and $(b_i, x_j + \frac{\pi}{4})$ respectively.
4. s_i in sector 2 and s_j in sector 5; therefore, in the new candidate pair, the i th and j th components will be $(b_j, x_i - \frac{\pi}{4})$ and $(b_i, x_j - \frac{\pi}{4})$ respectively.



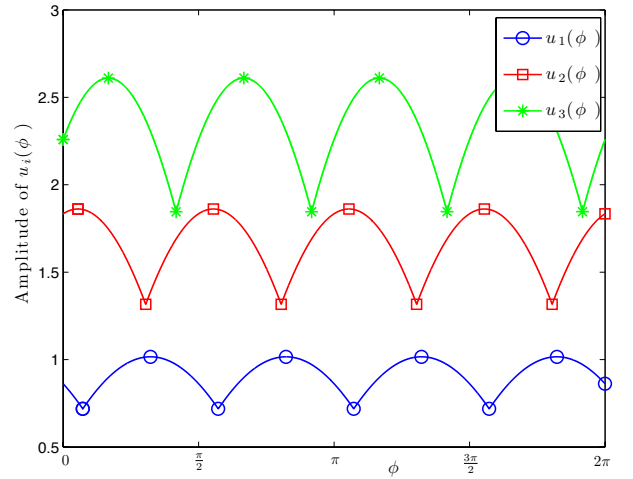
(a) Curves $u_n(\phi)$, $n = 1, 2, 3$, in the entire Φ , considering phase-only changes.



(c) Candidate pairs for subproblem \mathcal{P}_0 .



(b) Curves $u_n(\phi)$, $n = 1, 2, 3$, and the corresponding intersection points in $[0, \frac{\pi}{2}]$, considering phase-only changes.



(d) Illustration of $u_n(\phi)$, $n = 1, 2, 3$, for the candidate pairs in the entire Φ .

Figure 3: Example of solving subproblem \mathcal{P}_0 , considering $M = 8$, $L = 2$, and $N = 3$.

A new candidate pair, denoted by $(\mathbf{b}', \mathbf{x}')$, is obtained at some ϕ , say $\phi_{i,j}$. This implies that, for $\phi > \phi_{i,j}$,

$$\sum_{n=1}^N u'_n(\phi) > \sum_{n=1}^N u_n(\phi), \quad (31)$$

where $u_n(\phi)$ and $u'_n(\phi)$ originate from the candidate pairs (\mathbf{b}, \mathbf{x}) and $(\mathbf{b}', \mathbf{x}')$, respectively. The opposite

holds for $\phi < \phi_{i,j}$. Thus, $\phi_{i,j}$ can be obtained by solving, with respect to ϕ , the equation

$$\sum_{n=1}^N u'_n(\phi) = \sum_{n=1}^N u_n(\phi). \quad (32)$$

Notice that $N-2$ terms from (32) can be eliminated since the two candidate pairs share $N-2$ common components (b_n, x_n) . Therefore, (32) can be reduced to

$$\sum_{n=i,j} u_n(\phi) = \sum_{n=i,j} u'_n(\phi), \quad (33)$$

and, by solving with respect to ϕ , we obtain

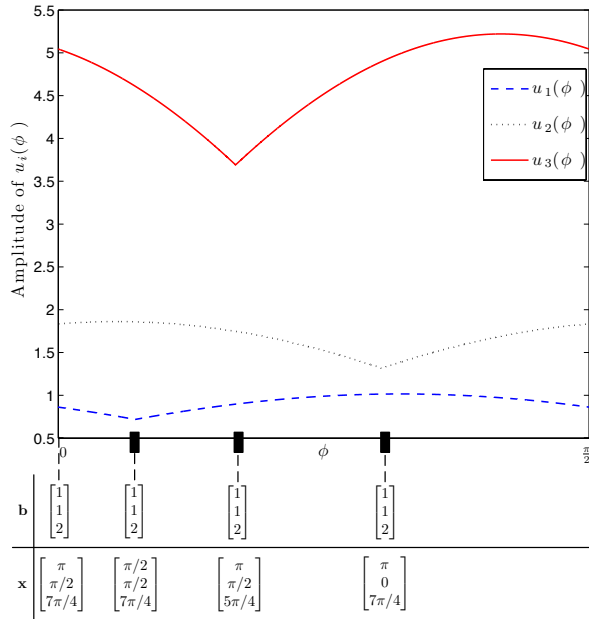
$$\phi_{i,j} = \tan^{-1} \left(\frac{b_i \mathbf{p} \mathbf{a}^T + b_j \mathbf{p} \mathbf{d}^T}{b_i \mathbf{p} \mathbf{c}^T + b_j \mathbf{p} \mathbf{r}^T} \right) \quad (34)$$

where,

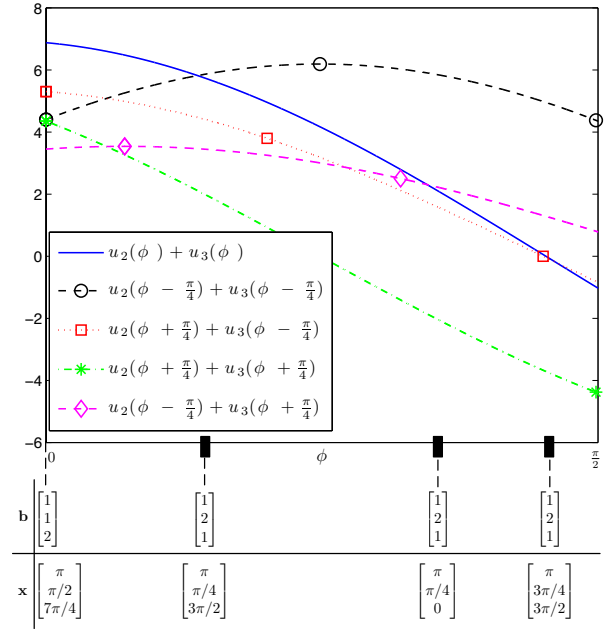
$$\begin{aligned} \mathbf{a} &= \begin{bmatrix} \sin x_i & \cos x_i & -\sin x'_j & -\cos x'_j \end{bmatrix}, \quad \mathbf{d} = \begin{bmatrix} -\sin x'_i & -\cos x'_i & \sin x_j & \cos x_j \end{bmatrix}, \\ \mathbf{c} &= \begin{bmatrix} -\cos x_i & \sin x_i & \cos x'_j & -\sin x'_j \end{bmatrix}, \quad \mathbf{r} = \begin{bmatrix} \cos x'_i & -\sin x'_i & -\cos x_j & \sin x_j \end{bmatrix}, \\ \mathbf{p} &= \begin{bmatrix} \Re\{y_i\} & \Im\{y_i^*\} & \Re\{y_j\} & \Im\{y_j^*\} \end{bmatrix}. \end{aligned}$$

Since x'_i and x'_j are taking two possible values, four values of $\phi_{i,j}$ are obtained through (34) for each pair i, j , as illustrated in Figs. 4b and 4c. All possible pairs i, j with $i \neq j$ are upper bounded by $\binom{N}{2} = \frac{N^2 - N}{2}$. Hence, each set \mathcal{G} is formed with complexity $\mathcal{O}(N^2)$, the elements of which are the ϕ 's that originate from all the possible phase-and-amplitude changes. In conjunction with the N values of ϕ that have been obtained from phase-only changes (as illustrated in Fig. 4a), we finally have $\mathcal{O}(N^2)$ values of ϕ in each set \mathcal{G} . Hence, the proposed algorithm requires $\mathcal{O}(N^2)$ operations to construct a set \mathcal{G} of cardinality less than or equal to $2N^2 - N$. Clearly, the number of these sets (or, equivalently, the number of $\phi^{(j)}$) will determine the overall complexity of solving \mathcal{P}_k , $\forall k = 1, 2, \dots, K-1$.

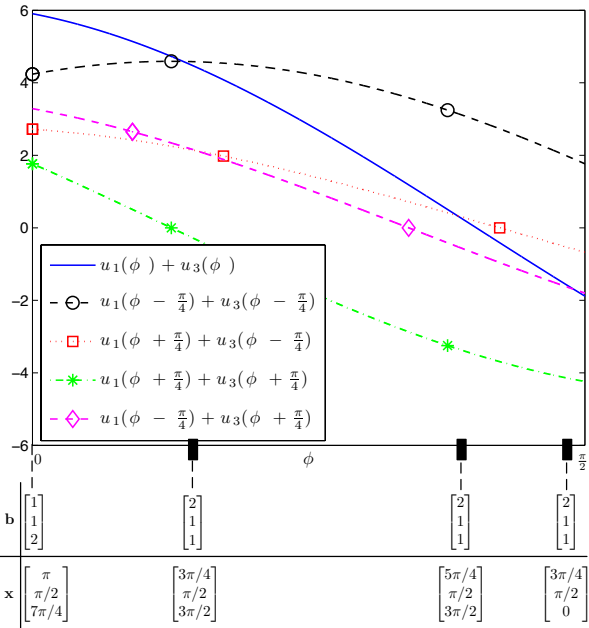
Using Lemma 2, we conclude that, if the candidate pair at $\phi = 0$ is (\mathbf{b}, \mathbf{x}) , then the candidate pair at $\phi = \frac{4\pi}{M}$ will be $(\mathbf{b}, \mathbf{x} - 4\pi/M)$. Thus, in order to upper bound the number of $\phi^{(j)}$, and consequently the cardinality of candidate pairs in each subproblem, it suffices to enumerate all the



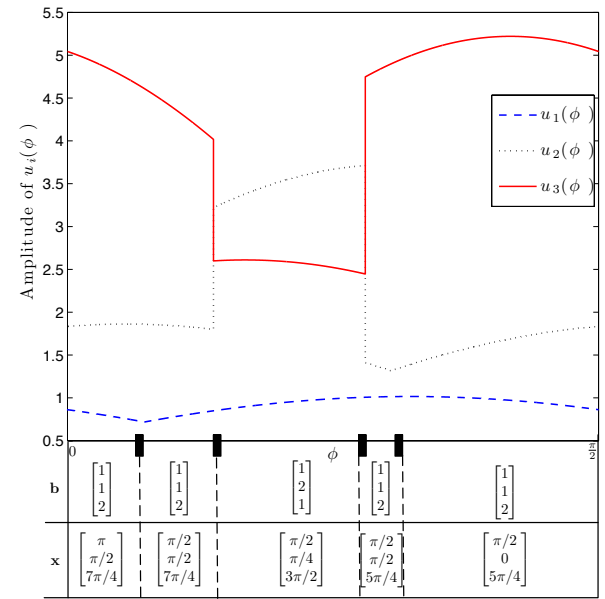
(a) Curves $u_n(\phi)$, $n = 1, 2, 3$, and the corresponding intersection points in $[0, \frac{\pi}{2})$, considering phase-only changes.



(c) Curves $u_n(\phi)$, $i = 2, 3$, and the corresponding intersection points in $[0, \frac{\pi}{2})$, considering phase-and-amplitude changes.



(b) Curves $u_n(\phi)$, $n = 1, 3$, and the corresponding intersection points in $[0, \frac{\pi}{2})$, considering phase-and-amplitude changes.



(d) Candidate pairs for subproblem \mathcal{P}_1 , and the corresponding $u_n(\phi)$, $n = 1, 2, 3$, for these pairs.

Figure 4: Example of solving \mathcal{P}_1 , considering $M = 8$, $L = 2$, and $N = 3$.

possible changes that result in the pair $(\mathbf{b}, \mathbf{x} - 4\pi/M)$ starting from (\mathbf{b}, \mathbf{x}) . The phase-only changes are $\mathcal{O}(N)$ and we consider the phase-and-amplitude changes. In the Appendix, considering the phases

of two components (b_i, x_i) , (b_j, x_j) of the candidate pair at $\phi = 0$ such that, $(b_i, x_i) \in \mathcal{B}_m \times \mathcal{X}_m$ and $(b_j, x_j) \in \mathcal{B}_n \times \mathcal{X}_n$ where $m \neq n$, we show that the phase-and-amplitude changes between the components i, j with $i, j \in \{1, 2, \dots, N\}$ are upper bounded by a constant, say c . This implies that, for the $\binom{N}{2}$ combinations of i, j of a candidate pair, the phase-and-amplitude changes are also upper bounded by $\binom{N}{2}c = \frac{N(N-1)}{2}c$. Therefore, since we have $\mathcal{O}(N^2)$ values of $\phi^{(j)}$, we obtain that \mathcal{P}_k , $\forall k = 1, 2, \dots, K - 1$, is solvable with complexity $\mathcal{O}(N^4)$. Since, due to Lemma 1, the number of subproblems K is polynomial in N , we conclude that problem \mathcal{P} is polynomially solvable. This completes the proof of Proposition 1.

In the Appendix, the transitions from one column to the next one indicate a phase-and-amplitude change, hence from (34) four outcomes should be considered in each transition. However, many of the outcomes are eliminated due to invalid phase change and are denoted with a slash in the Appendix. For instance, for the case of $M = 8$, consider the path

$$\begin{bmatrix} b_i \\ b_j \end{bmatrix} \begin{bmatrix} x_i \\ x_j \end{bmatrix} \longrightarrow \begin{bmatrix} b_j \\ b_i \end{bmatrix} \begin{bmatrix} x_i + \pi/4 \\ x_j - \pi/4 \end{bmatrix} \longrightarrow \begin{bmatrix} b_i \\ b_j \end{bmatrix} \begin{bmatrix} x_i + \pi/2 \\ x_j - \pi/2 \end{bmatrix}. \quad (35)$$

In (35), the amplitude component is also illustrated in contrast to Appendix due to limited space. We focus on phase x_i and, utilizing Fig. 2a, we notice that x_i cannot end up in sectors 7 or 8 starting from sectors 1 or 2 since the phase is rotated clockwise and cannot exceed a rotation by $\frac{\pi}{2}$. The upper bound on phase-and-amplitude changes, c , can be obtained considering the longest path in the Appendix. However, along a path, the same pair can be appeared more than once. Thus, in order to derive an upper bound in transitions, we need to ensure that there is no loop. Indeed, if certain phase-and-amplitude changes have been occurred, then they should not be taken into consideration again due to the constraints in (28). To be more specific, consider the following path

$$\begin{bmatrix} b_m \\ b_n \end{bmatrix} \begin{bmatrix} x_m \\ x_n \end{bmatrix} \xrightarrow{\phi^{(1)}} \begin{bmatrix} b_n \\ b_m \end{bmatrix} \begin{bmatrix} x_m - 2\pi/M \\ x_n - 2\pi/M \end{bmatrix} \xrightarrow{\phi^{(2)}} \begin{bmatrix} b_m \\ b_n \end{bmatrix} \begin{bmatrix} x_m \\ x_n \end{bmatrix}. \quad (36)$$

Due to (28), $\phi^{(1)}$ is less than $\phi^{(2)}$ and $\phi^{(3)}$ should be strictly greater than $\phi^{(2)}$. Consequently, $\phi^{(3)}$ cannot equal $\phi^{(1)}$, implying that the phase-and-amplitude changes which have already occurred cannot occur again. Thus, another path should be followed and, since the choices are bounded, the transitions

will be bounded too, resulting in the conclusion that the cardinality of $\phi^{(j)}$ is bounded.

4 The Proposed Algorithm

In this section, we present the complete proposed algorithm, for the case of $L = 2$, that finds all the optimal pairs (\mathbf{b}, \mathbf{x}) for each subproblem \mathcal{P}_k , $\forall k = 0, 1, \dots, K$, or, equivalently, the optimal vector $\mathbf{s} \in \mathcal{A}^N$ for the initial problem \mathcal{P} . The pseudo-code is presented in Fig. 5 and is divided into three main sections. The construction of the optimal pair at $\phi = 0$ at lines 2–16, the construction of each set \mathcal{G}_j , $\forall j$, and the calculation of the values of ϕ 's that originate from phase-only changes and phase-and-amplitude changes at lines 20–22 and 24–33, respectively, and, finally, the selection of proper $\phi^{(j)}$ at lines 34–45.

At lines 2–8, we form the two triplets $(\mathbf{b}^{(1)}, \mathbf{x}^{(1)}, \mathbf{u}^{(1)})$ and $(\mathbf{b}^{(2)}, \mathbf{x}^{(2)}, \mathbf{u}^{(2)})$ with complexity $\mathcal{O}(NM)$ and then, at lines 9–10, the vector \mathbf{g} is formed and is sorted with complexity $\mathcal{O}(N)$ and $\mathcal{O}(N \log N)$, respectively. For each subproblem \mathcal{P}_k , at line 11, we pick the k indexes from the sorting procedure at line 10 which correspond to the k greatest values of \mathbf{g} and we form the candidate pair (\mathbf{b}, \mathbf{x}) at $\phi = 0$ by setting to the k positions of \mathbf{b} and \mathbf{x} , at lines 13–16, the corresponding values from $\mathbf{b}^{(2)}$ and $\mathbf{x}^{(2)}$, respectively, with complexity $\mathcal{O}(N)$.

At lines 20–22, we calculate the values of ϕ in which all the next candidate optimal pairs are formed, considering phase-only changes. This procedure is accomplished with complexity $\mathcal{O}(N)$ and then, at lines 24–33, we calculate the values of ϕ in which all the next candidate pairs are formed, considering phase-and-amplitude changes. For each one among the at most $\binom{N}{2}$ combinations of line 25, we have to compute, as mentioned in Subsection 3.3, four possible phase combinations (line 29), i.e., $(x_i + 2\pi/M, x_j + 2\pi/M)$, $(x_i - 2\pi/M, x_j + 2\pi/M)$, $(x_i - 2\pi/M, x_j - 2\pi/M)$ and $(x_i + 2\pi/M, x_j - 2\pi/M)$, which result in the computation of four distinct values of ϕ .

Thus, with $4\binom{N}{2} + N = 2N^2 - N$ operations, we obtain all the values of ϕ in which all the candidate pairs ($\mathcal{O}(N^2)$ in cardinality) are formed and, at line 34, with complexity $\mathcal{O}(N^2)$ we pick $\phi^{(j)}$ from set \mathcal{G}_j and, consequently, the corresponding optimal pair for the particular ϕ . Then, at lines 36–45, we apply the changes to the previous optimal pair in order to obtain the new one. At lines 38–39, we change only the phase if $\phi^{(j)}$ corresponds to a phase-only change and, respectively, at lines 41–44 we apply the phase-and-amplitude changes.

Therefore, with complexity $\mathcal{O}(N^2)$, a new candidate pair has been obtained and the above procedure should be repeated until we scan the entire range $[0, \frac{4\pi}{M})$. The number of iterations (line 18), as shown in 3.3, is upper bounded by $\mathcal{O}(N^2)$ resulting in the overall complexity of $\mathcal{O}(N^4)$ to solve subproblems \mathcal{P}_k , $k = 1, 2, 3, \dots, K - 1$. Subproblems \mathcal{P}_0 and \mathcal{P}_K require $\mathcal{O}(N)$ computations since only lines 20–22 should be considered. Finally, since the cardinality of the subproblems is $\mathcal{O}(N)$ and the required calculations are $\mathcal{O}(N^4)$, the candidate pairs for all subproblems \mathcal{P}_k are formed with complexity $\mathcal{O}(N^5)$. Equivalently, vectors $\mathbf{s} \in \mathcal{A}^N$ are formed through $\mathbf{s} = \mathbf{b} \odot e^{j\mathbf{x}}$. The latter are applied in (11) and we keep the vector \mathbf{s} which results in the greatest metric value.

```

1:  $\mathbf{V} \leftarrow [\Re(\mathbf{y}) \Im(\mathbf{y}^*)]$ 
2: for  $i = 1 : 2$  do
3:   for  $j = 1 : N$  do
4:     find  $x_j \in \mathcal{X}_i$  s.t.  $b_{i,j}(V_{j,1} \sin(x_j) + V_{j,2} \cos(x_j))$  is maximized, and then
5:      $x_j^{(i)} \leftarrow x_j$ ;
6:      $u_j^{(i)} \leftarrow b_j^{(i)}(V_{j,1} \sin(x_j) + V_{j,2} \cos(x_j))$ ;
7:   end for
8: end for
9:  $\mathbf{g} \leftarrow \mathbf{u}^{(2)} - \mathbf{u}^{(1)}$ ;
10:  $[\text{indexes}, \text{values}] \leftarrow \text{sort}[g_1, g_2, \dots, g_N]$ ;
11: for  $k = 0 : K$  do
12:    $\phi^{(0)} \leftarrow 0$ ;
13:    $\mathbf{b}^{(k,0)} \leftarrow \mathbf{b}^{(1)}$ ;
14:    $\mathbf{x}^{(k,0)} \leftarrow \mathbf{x}^{(1)}$ ;
15:    $\mathbf{b}_{\text{indexes}(1:k)}^{(k,0)} \leftarrow \mathbf{b}_{\text{indexes}(1:k)}^{(2)}$ ;
16:    $\mathbf{x}_{\text{indexes}(1:k)}^{(k,0)} \leftarrow \mathbf{x}_{\text{indexes}(1:k)}^{(2)}$ ;
17:    $j \leftarrow 0$ ;
18:   while  $\phi^{(j)} < \frac{4\pi}{M}$  do
19:      $j \leftarrow j++$ ;
20:     for  $i = 1 : N$  do
21:        $\phi_i \leftarrow \text{calc. through Eq. (30)}$ ;
22:     end for
23:      $i \leftarrow 1$ ;
24:     if  $k \neq 1, K$  then
25:       for  $m, n \in \{1, 2, \dots, N\}$  with  $m \neq n$  do
26:         for  $p = 1 : 4$  do
27:            $\phi_{N+i} \leftarrow \text{calc. through Eq. (34)}$ ;
28:            $\text{ampl}[k, p] \leftarrow [m, n]$ ;
29:            $\text{phases}[k, p] \leftarrow [x_m^{(k,j-1)} \pm 2\pi/M, x_n^{(k,j-1)} \pm 2\pi/M]$ ;
30:            $i \leftarrow i++$ ;
31:         end for
32:       end for
33:     end if
34:     pick index  $l$  from the set  $\mathcal{G}_j = \{\phi_1, \dots, \phi_N, \phi_{N+1}, \dots, \phi_{\mathcal{O}(N^2)}\}$  according to Eq. (28);
35:      $\phi^{(j)} \leftarrow \phi_l$ ;
36:      $\mathbf{b}^{(k,j)} \leftarrow \mathbf{b}^{(k,j-1)}$ ;
37:      $\mathbf{x}^{(k,j)} \leftarrow \mathbf{x}^{(k,j-1)}$ ;
38:     if  $l \leq N$  then
39:        $x_l^{(k,j)} \leftarrow x_l^{(k,j-1)} - 4\pi/M$ ;
40:     else
41:       from the arrays  $\text{ampl}$  and  $\text{phases}$  retrieve the corresponding change and apply
42:       Swap  $b_m^{(k,j)}$  with  $b_n^{(k,j)}$ ;
43:        $x_m^{(k,j)} \leftarrow x_m^{(k,j-1)} \pm 2\pi/M$ ;
44:        $x_n^{(k,j)} \leftarrow x_n^{(k,j-1)} \pm 2\pi/M$ ;
45:     end if
46:   end while
47: end for

```

Figure 5: The proposed algorithm for optimal blind APSK sequence detection with $L = 2$ amplitude levels.

5 Extension to the general case of $L > 2$

To simplify the presentation, we thoroughly discussed the case of $L = 2$ and arbitrary M . Nevertheless, by slightly modifying the presented algorithm in Fig. 5, it still solves, with polynomial complexity in N , the general case where $L > 2$. The subproblems are still $K = \mathcal{O}(N^{L-1})$ and the candidate pairs at $\phi = 0$ for each subproblem can be obtained following the same procedure as in case of $L = 2$. However, $L - 1$ vectors \mathbf{g} need to be constructed such that $\mathbf{g}_l = \mathbf{u}^{(l+1)} - \mathbf{u}^{(1)}$, $\forall l = 1, 2, \dots, L - 1$. The candidate pair at $\phi = 0$ for each subproblem \mathcal{P}_k , $k = 0, 1, \dots, K$, is obtained by solving the integer programming problem

$$\begin{aligned} & \underset{\mathbf{i}}{\text{minimize}} && -\mathbf{f}^T \mathbf{i} \\ & \text{s.t.} && \mathbf{A}_{eq} \mathbf{i} = \mathbf{c}_{eq}, \\ & && \mathbf{A} \mathbf{i} \leq \mathbf{c} \end{aligned} \tag{37}$$

where

$$\mathbf{A}_{eq} = \begin{bmatrix} \mathbf{1}_{1 \times N} & \mathbf{0}_{1 \times N} & \cdots & \mathbf{0}_{1 \times N} \\ \mathbf{0}_{1 \times N} & \mathbf{1}_{1 \times N} & \cdots & \mathbf{0}_{1 \times N} \\ \vdots & \vdots & \ddots & \vdots \\ \mathbf{0}_{1 \times N} & \mathbf{0}_{1 \times N} & \cdots & \mathbf{1}_{1 \times N} \end{bmatrix}_{(L-1) \times N(L-1)}, \quad \mathbf{A} = \begin{bmatrix} \mathbf{I}_N & \cdots & \mathbf{I}_N \end{bmatrix}_{N \times N(L-1)}, \quad \mathbf{c} = \mathbf{1}_{N \times 1},$$

and vector \mathbf{f} contains vectors \mathbf{g}_l , $\forall l = 1, 2, \dots, L - 1$, concatenated, i.e., $\mathbf{f} = [\mathbf{g}_1^T, \mathbf{g}_2^T, \dots, \mathbf{g}_{L-1}^T]^T_{N(L-1) \times 1}$. The elements of vector \mathbf{c}_{eq} are the last $L - 1$ elements of vector \mathbf{t}_k , $\forall k = 0, 1, \dots, K$, that has been defined in Subsection 3.1. The second constraint in (37) is used to ensure that each component of the candidate pair will belong exclusively in $\mathcal{B}_l \times \mathcal{X}_l$ for some $l = 1, 2, \dots, L$. Since the constraint matrices \mathbf{A}_{eq} and \mathbf{A} are totally unimodular, the solution of (37) exists and is guaranteed to be integral. Moreover, due to total unimodularity, the integer problem can be solved in polynomial time by solving the linear programming relaxation [34]. Thus, with polynomial complexity, we obtain the binary vector $\mathbf{i}_{N(L-1) \times 1}$, the elements of which indicate the components of the optimal pair at $\phi = 0$ for each subproblem.

Due to the definition in (1), whenever $L > 2$, candidate pairs (\mathbf{b}, \mathbf{x}) are created also by considering amplitude-only changes. Consider a candidate optimal pair (\mathbf{b}, \mathbf{x}) at some ϕ and two of its components,

namely $(b_i, x_i) \in \mathcal{B}_k \times \mathcal{X}_k$ and $(b_j, x_j) \in \mathcal{B}_l \times \mathcal{X}_l$ such that k, l are either even or odd, and $k \neq l$. Notice that

$$\begin{aligned} \mathcal{X}_1 = \mathcal{X}_3 = \dots = \mathcal{X}_L \text{ and } \mathcal{X}_2 = \mathcal{X}_4 = \dots = \mathcal{X}_{L-1}, \text{ if } L \text{ is odd} \\ \text{or} \\ \mathcal{X}_1 = \mathcal{X}_3 = \dots = \mathcal{X}_{L-1} \text{ and } \mathcal{X}_2 = \mathcal{X}_4 = \dots = \mathcal{X}_L, \text{ if } L \text{ is even.} \end{aligned} \quad (38)$$

Thus, a change of the form $(b_i, x_i) \rightarrow (b_j, x_j)$ and $(b_j, x_j) \rightarrow (b_i, x_i)$ is valid and should be considered as well. The new candidate pair $(\mathbf{b}', \mathbf{x}')$ can be easily obtained by setting $(\mathbf{b}', \mathbf{x}') = (\mathbf{b}, \mathbf{x})$ and exchanging the i th with the j th amplitude component of \mathbf{b}' . The value of ϕ , in which this candidate pair is formed, can be obtained by solving, with respect to ϕ , the equality

$$\sum_{n=i,j} u_n(\phi) = \sum_{n=i,j} u'_n(\phi) \quad (39)$$

where $u_n(\phi)$ and $u'_n(\phi)$ originate from the candidate pairs (\mathbf{b}, \mathbf{x}) and $(\mathbf{b}', \mathbf{x}')$, respectively. The value of ϕ that satisfies equation (39) is given by

$$\phi = \tan^{-1} \left(\frac{-\Re\{y_j\} \sin x_j - \Im\{y_j^*\} \cos x_j + \Re\{y_i\} \sin x_i + \Im\{y_i^*\} \cos x_i}{\Re\{y_j\} \cos x_j - \Im\{y_j^*\} \sin x_j - \Re\{y_i\} \cos x_i + \Im\{y_i^*\} \sin x_i} \right). \quad (40)$$

Sets \mathcal{G} are still of size $\mathcal{O}(N^2)$ and, thus, we find the $\phi^{(j)}$ for each set \mathcal{G}_j in $\mathcal{O}(N^2)$ time complexity. However, whenever phase-and-amplitude changes or phase-only changes are considered, sorting should be applied too. Sorting is employed in order to assign, in a maximal-ratio-combining sense, the components of \mathbf{b} to the components of \mathbf{x} in positions \mathbf{i} , where \mathbf{i} is defined as

$$\mathbf{i} \triangleq \{i \in \{1, \dots, N\} : x_i, x_j \in \mathcal{X}_l \text{ for some } l \in \{1, \dots, L\}, \text{ and } \forall j \in \{1, \dots, N\} \text{ where } j \neq i\}. \quad (41)$$

Hence, the proposed algorithm needs $\mathcal{O}(N^2 \log N)$ operations to obtain the next candidate pair and in each subproblem the cardinality of these pairs is $\mathcal{O}(N^2)$. The latter is true since, by using Appendix with a slight modification, due to the amplitude changes, the changes between any component pair are upper bounded by a constant, similar to the case of $L = 2$. In each valid “state” along a path, there is an additional transition that is a self-transition from each “state” to itself, implying an amplitude

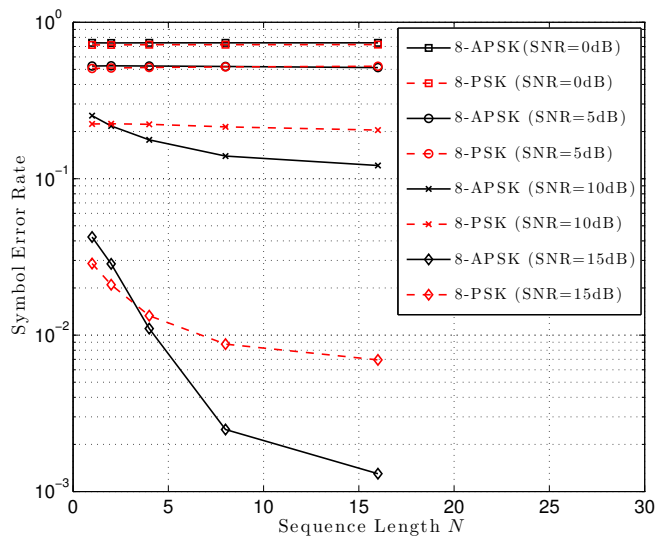
change. In conclusion, each subproblem is solvable in polynomial time and, since the cardinality of the subproblems is $\mathcal{O}(N^{L-1})$, (11) is solvable in polynomial time for the general case of $L > 2$.

6 Simulation Results

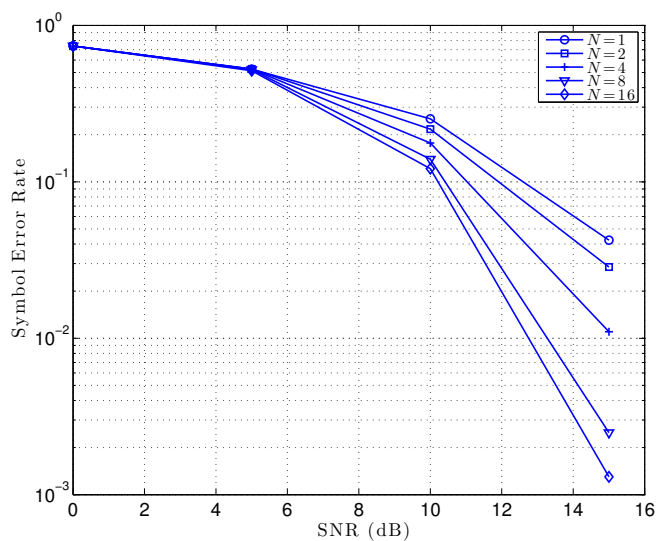
To illustrate the performance of the proposed polynomial-complexity implementation of the optimal blind APSK sequence detector, we consider APSK transmissions over an unknown channel. In addition, to realize the benefits of our algorithm as the sequence length increases and the channel phase changes, we fix the channel amplitude and consider a uniform channel-phase distribution (as, for example, in the Rayleigh-fading case). Moreover, to avoid channel phase ambiguities, we employ differential encoding, as it was presented in [2] but without imposing energy constraints. ML-optimal sequence detection is employed by the receiver and the presented results are averaged over 10^5 symbol transmissions drawn from an 8-APSK constellation.

In Fig. 6a, we plot the symbol error rate (SER) as a function of the sequence length N , for differentially encoded 8-APSK and differentially encoded 8-PSK, by setting the signal-to-noise ratio (SNR) to 0dB, 5dB, 10dB, and 15dB. We observe the superiority of APSK (when decoded with the proposed algorithm) which increases with the sequence length.

Fig. 6b presents SER as a function of SNR for 8-APSK. We note that, for a sequence length $N = 16$, the conventional exhaustive-search approach would require $8^{16} = 2^{48}$ computations to perform optimal blind APSK detection, while the proposed algorithm achieves the same optimal performance with polynomial complexity.



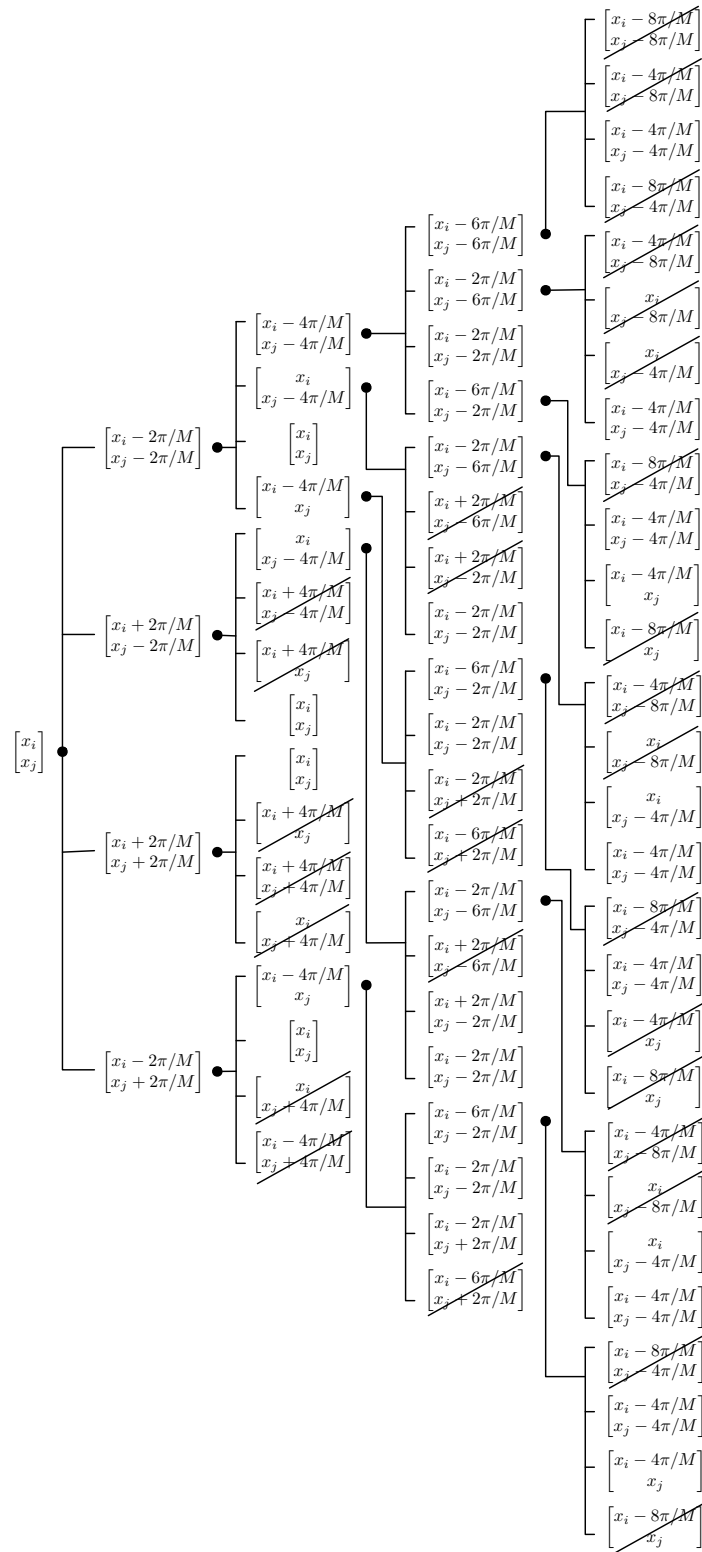
(a) SER versus sequence length N for differentially encoded 8-APSK with $r_1 = 1$ and $r_2 = 2$ and differentially encoded 8-PSK.



(b) SER versus SNR for differentially encoded 8-APSK with $r_1 = 1$ and $r_2 = 2$.

Figure 6: ML noncoherent receivers for various values of SNR and sequence length N .

7 Appendix



References

- [1] R. De Gaudenzi, A. Guillén i Fàbregas, A. Martinez, and B. Ponticelli, “High power and spectral efficiency coded digital modulation schemes for nonlinear satellite channels,” in *Proc. ESA 7th Int. Workshop on DSP Applied to Space Commun.*, Sesimbra, Portugal, Oct. 2001, CD-ROM.
- [2] D. Warrier and U. Madhow, “Spectrally efficient noncoherent communication,” *IEEE Trans. Inf. Theory*, vol. 48, no. 3, pp. 651–668, Mar. 2002.
- [3] X.-G. Xia, “Differentially en/decoded orthogonal space–time block codes with APSK signals,” *IEEE Commun. Letters*, vol. 6, no. 4, pp. 150–152, Apr. 2002.
- [4] R.-R. Chen, R. Koetter, U. Madhow, and D. Agrawal, “Joint noncoherent demodulation and decoding for the block fading channel: a practical framework for approaching Shannon capacity,” *IEEE Trans. Commun.*, vol. 51, no. 10, pp. 1676–1689, Oct. 2003.
- [5] L. Giugno, M. Luise, and V. Lottici, “Adaptive pre- and post-compensation of nonlinear distortions for high-level data modulations,” *IEEE Trans. Wireless Commun.*, vol. 3, no. 5, pp. 1490–1495, Sep. 2004.
- [6] Y. Ma, Q. T. Zhang, R. Schober, and S. Pasupathy, “Diversity reception of DAPSK over generalized fading channels,” *IEEE Trans. Wireless Commun.*, vol. 4, no. 4, pp. 1834–1846, Jul. 2005.
- [7] G. Albertazzi, S. Cioni, G. E. Corazza, M. Neri, R. Pedone, P. Salmi, A. Vanelli-Coralli, and M. Villanti, “On the adaptive DVB-S2 physical layer: design and performance,” *IEEE Wireless Commun.*, vol. 12, no. 6, pp. 62–68, Dec. 2005.
- [8] R. De Gaudenzi, A. Guillén i Fàbregas, and A. Martinez, “Performance analysis of Turbo-coded APSK modulations over nonlinear satellite channels,” *IEEE Trans. Wireless Commun.*, vol. 5, no. 9, pp. 2396–2407, Sep. 2006.
- [9] R.-Y. Wei, T.-C. Sue, H.-H. Wang, and C.-S. Wang, “Noncoherent block-coded QAM,” in *Proc. IEEE Int. Conf. on Commun.*, Glasgow, UK, Jun. 2007, pp. 863–869.

- [10] R.-Y. Wei, S.-S. Gu, and T.-C. Sue, “Noncoherent block-coded TAPSK,” *IEEE Trans. Commun.*, vol. 57, no. 11, pp. 3195–3198, Nov. 2009.
- [11] R.-Y. Wei, T.-S. Lin, and S.-S. Gu, “Block-coded 16QAM for noncoherent decoding,” in *Proc. IEEE Wireless Commun. and Networking Conf.*, Sydney, Australia, Apr. 2010, pp. 1–6.
- [12] R.-Y. Wei, T.-S. Lin, and S.-S. Gu, “Noncoherent block-coded TAPSK and 16QAM using linear component codes,” *IEEE Trans. Commun.*, vol. 58, no. 9, pp. 2493–2498, Sep. 2010.
- [13] R.-Y. Wei, “Differential encoding by a look-up table for quadrature-amplitude modulation,” *IEEE Trans. Commun.*, vol. 59, no. 1, pp. 84–94, Jan. 2011.
- [14] Z. Liu, Q. Xie, K. Peng, and Z. Yang, “APSK constellation with gray mapping,” *IEEE Commun. Letters*, vol. 15, no. 12, pp. 1271–1273, Dec. 2011.
- [15] D. Makrakis and P. T. Mathiopoulos, “Optimal decoding in fading channels: A combined envelope, multiple differential and coherent detection approach,” in *Proc. IEEE Global Commun. Conf.*, Dallas, TX, Nov. 1989, vol. 3, pp. 1551–1557.
- [16] S. G. Wilson, J. Freebersyser, and C. Marshall, “Multi-symbol detection of M-DPSK,” in *Proc. IEEE Global Commun. Conf.*, Dallas, TX, Nov. 1989, vol. 3, pp. 1692–1697.
- [17] D. Divsalar and M. K. Simon, “Multiple-symbol differential detection of MPSK,” *IEEE Trans. Commun.*, vol. 38, no. 3, pp. 300–308, Mar. 1990.
- [18] H. Leib and S. Pasupathy, “Noncoherent block demodulation of PSK,” in *Proc. 40th IEEE Veh. Technol. Conf.*, Orlando, FL, May 1990, pp. 407–411.
- [19] T. L. Marzetta and B. M. Hochwald, “Capacity of a mobile multiple-antenna communication link in rayleigh flat fading,” *IEEE Trans. Inf. Theory*, vol. 45, no. 1, pp. 139–157, Jan. 1999.
- [20] L. Zheng and D. N. C. Tse, “Communication on the Grassmann manifold: A geometric approach to the noncoherent multiple-antenna channel,” *IEEE Trans. Inf. Theory*, vol. 48, no. 2, pp. 359–383, Feb. 2002.

- [21] K. Mackenthun, “A fast algorithm for maximum likelihood detection of QPSK or $\pi/4$ -QPSK sequences with unknown phase,” in *Proc. IEEE Third Intern. Symp. on Personal, Indoor and Mobile Radio Commun.*, Boston, MA, Oct. 1992, pp. 240–244.
- [22] K. M. Mackenthun, Jr., “A fast algorithm for multiple-symbol differential detection of MPSK,” *IEEE Trans. Commun.*, vol. 42, no. 2/3/4, pp. 1471–1474, Feb./Mar./Apr. 1994.
- [23] W. Sweldens, “Fast block noncoherent decoding,” *IEEE Commun. Letters*, vol. 5, no. 4, pp. 132–134, Apr. 2001.
- [24] I. Motedayen-Aval, A. Krishnamoorthy, and A. Anastasopoulos, “Optimal joint detection/estimation in fading channels with polynomial complexity,” *IEEE Trans. Inf. Theory*, vol. 53, no. 1, pp. 209–223, Jan. 2007.
- [25] G. N. Karystinos and D. A. Pados, “Rank-2-optimal adaptive design of binary spreading codes,” *IEEE Trans. Inf. Theory*, vol. 53, no. 9, pp. 3075–3080, Sep. 2007.
- [26] I. Motedayen-Aval and A. Anastasopoulos, “Polynomial-complexity noncoherent symbol-by-symbol detection with application to adaptive iterative decoding of Turbo-like codes,” *IEEE Trans. Commun.*, vol. 51, no. 2, pp. 197–207, Feb. 2003.
- [27] D. J. Ryan, I. B. Collings, and I. V. L. Clarkson, “GLRT-optimal noncoherent lattice decoding,” *IEEE Trans. Signal Process.*, vol. 55, no. 7, pp. 3773–3786, Jul. 2007.
- [28] R. G. McKilliam, D. J. Ryan, I. V. L. Clarkson, and I. B. Collings, “An improved algorithm for optimal noncoherent QAM detection,” in *Proc. IEEE Austral. Commun. Theory Workshop*, Christchurch, New Zealand, Feb. 2008, pp. 64–68.
- [29] D. S. Papailiopoulos, G. A. Elkheir, and G. N. Karystinos, “Maximum-likelihood noncoherent PAM detection,” *IEEE Trans. Commun.*, vol. 61, no. 3, pp. 1152–1159, Mar. 2013.
- [30] R. G. McKilliam, D. J. Ryan, V. L. Clarkson, and I. B. Collings, “Block noncoherent detection of hexagonal QAM,” in *Proc. IEEE Austral. Commun. Theory Workshop*, Canberra, ACT, Feb. 2010, pp. 65–70.
- [31] C. D. Meyer, *Matrix Analysis and Applied Linear Algebra*. Philadelphia, PA: SIAM, 2000.

- [32] T. M. Cover and J. A. Thomas, *Elements of Information Theory*, 2nd edition. New York, NY: Wiley, 2006.
- [33] R. P. Stanley, *Enumerative Combinatorics, Volume 1*, 2nd edition. New York, NY: Cambridge University Press, 2012.
- [34] D. S. Hochbaum, “Network flows and graphs,” *Course notes, Lectures 1–5*, University of California, Berkeley, Aug. 28 – Sep. 11, 2008, url:<http://www.ieor.berkeley.edu/~ieor266/Lecture1-5.pdf> .